Applied Physics Letters

Subthermionic negative capacitance ion sensitive field-effect transistor

Cite as: Appl. Phys. Lett. **116**, 173503 (2020); https://doi.org/10.1063/5.0005411
Submitted: 20 February 2020 . Accepted: 15 April 2020 . Published Online: 28 April 2020

Francesco Bellando, Chetan K. Dabhi, Ali Saeidi, Carlotta Gastaldi, Yogesh S. Chauhan, and Adrian M. Ionescu

Applied Physics Letters ARTICLE scitation.org/journal/apl

Subthermionic negative capacitance ion sensitive field-effect transistor

Cite as: Appl. Phys. Lett. **116**, 173503 (2020); doi: 10.1063/5.0005411
Submitted: 20 February 2020 · Accepted: 15 April 2020 ·
Published Online: 28 April 2020

Francesco Bellando,[1,a] Chetan K. Dabhi,[2] Ali Saeidi,[1] Carlotta Gastaldi,[1] Yogesh S. Chauhan,[2] and Adrian M. Ionescu[1,a]

AFFILIATIONS

[1]Ecole Polytechnique Federale de Lausanne, Route Cantonale, Lausanne 1015, Switzerland
[2]Indian Institute of Technology, Kalyanpur, Kanpur, Uttar Pradesh 208 016, India

[a]Authors to whom correspondence should be addressed: francesco.bellando@epfl.ch and adrian.ionescu@epfl.ch

ABSTRACT

One of the main advantages of Ion-Sensitive Field-Effect Transistor (ISFET) technology is the capability to exploit technological advancements initially developed for conventional FETs for logic applications, such as the employ of high-k dielectrics for the gate and the definition of fully depleted and gate all around structures. Negative Capacitance (NC) is an emerging concept exploiting ferroelectric materials integrated in field effect transistor gate stacks in order to decrease their subthreshold swing and improve the drain current (I_D) overdrive in order to reach more energy efficient devices, operated at lower voltage. In this work, we investigate and experimentally demonstrate the application of this concept to enable subthermionic ISFETs with enhanced current sensitivity and low power operation. A physical model for the introduced NC ISFET is presented and optimized by fitting of the experimental results, providing further insights into the sensor parameters and a predictive tool for the design of future NC-based sensors.

The advantages of Ion-Sensitive Field-Effect Transistors (ISFETs) related to high sensitivity and low power operation, low fabrication cost, and intrinsic Complementary Metal-Oxide-Semiconductor (CMOS) compatibility have been explored and demonstrated in many studies.[1–22]

The Nernst limit states that the voltage sensitivity (S_V), i.e., the variation of threshold voltage (V_{th}) due to a variation of one unit of pH (defined as $-\log[H^+]$, where $[H^+]$ is the concentration of hydrogen ions)[23] is limited to 60 mV at room temperature (300 K). In a Field Effect Transistor (FET), the minimum gate voltage (V_G) variation needed to achieve a 10× variation of I_D is imposed by the thermionic limit of 60 mV. Consequently, the current sensitivity (S_I) for a conventional ISFET cannot be larger than one decade of current per unit of pH. Recently, the Negative Capacitance (NC) effect shown by ferroelectric materials has been proposed to reduce the subthreshold slope (SS) of FETs below the thermionic limit.[24–28] Exploiting the NC region of ferroelectrics is difficult due to its instability. However, it can be stabilized if the ferroelectric capacitor (Fe-Cap) is placed in-series with an appropriate positive capacitor,[29] potentially the MOSFET with tunable gate capacitance. Until now, such NC configuration has been used for solid-state electronic devices but never for ISFETs, where the solid-state device is combined with an in-series Liquid Under Test (LUT).

In this study, we design, fabricate, and perform an experimental study on SOI ISFETs connected with Fe-Caps to demonstrate that NC effect can significantly improve the S_I of conventional ISFETs by reducing their SS below the thermionic limit.

A physical model for the capacitance of the liquid gate (LG) is introduced and integrated in a SPICE (Simulation Program with Integrated Circuit Emphasis) simulation environment, which is calibrated from experimental data for the transfer characteristics. The resulting model is used to evaluate and investigate the impact of additional system parameters, such as the increase in the overall gate capacitance, which helps increasing the Signal to Noise Ratio (SNR) by reducing the flicker noise. This work reports the experimental characterization of an NC ISFET device and the definition of a predictive physical model capable of explaining and offering excellent agreement with measurement results. Some prior ideas of using an NC FET as sensing elements have been reported under the form of patents;[30,31] however, none of these patents report any similar experimental demonstration of NC effect in a ISFET.

Three sets of Fe-Caps [a 46 nm thick single-crystalline Pb(Zr,Ti)O3 (PZT) and two types of 16 nm thick Si-doped HfO_2 with

different annealing temperatures] are studied. In the proposed configuration, the Fe-Cap is connected between the MOSFET gate and a platinum electrode with an area of 2 mm^2 in contact with the LG. The Fully Depleted (FD) SOI MOSFET has a 20 nm thick buried oxide (BOx), 30 nm thick silicon layer, and a gate stack composed of 3 nm of HfO_2 on 5 nm of SiO_2; the intrinsic channel is 16 μm long and 6 μm wide and the metal gate is overlapping the N^+ doped contact regions by 3 μm per side. For the NC matching, we have designed and fabricated banks of Fe-Caps of various dimensions, similarly to a previous report,[32] and we built external connections between the backsides of Fe-Cap chips and MOSFET gate contacts on a different chip. The proof-of-concept for an NC ISFET is experimentally validated and tested by connecting its individual components (base FD SOI FET, Fe-Cap and sensing electrode). This is an efficient strategy for testing and optimizing the matching conditions with different sizes and materials for the Fe-Caps. It also permits to compare and evaluate the SS improvement given by the NC effect since it allows comparing the transfer characteristics of the very same ISFET *with* and *without* the ferroelectric component.

In Ferroelectric Metal Insulator Semiconductor (FMIS) structures, current leakages could discharge the polarization of the ferroelectric layer and jeopardize the NC effect.[33]

Significantly, recent papers[34,35] reported using pulsed measurements to study and substantiate NC effects in FMIS structures since a fast pulsed biasing and measuring permits investigation of the device response before leakage can discharge the capacitors. Therefore, in this work, we focused our experiments on pulsed mode characterization of NC ISFET.

Figure 1(a) suggests the expected benefits of a NC ISFET in terms of higher current sensitivity to a pH variation, compared to a conventional ISFET. When the ferroelectric capacitor, C_{FE}, is matched for gain and stabilized [Fig. 1(b)] in a series configuration with the capacitance of the LUT (C_{LUT}) and with the MOS capacitor (C_{MOS}), an internal voltage amplification is obtained ($dV_{INT}/dV_G \gg 1$). Note that the main difference compared with a subthermionic NC MOSFET used as a digital logic switch is that the conditions for NC also have to take into account the variable C_{LUT}, which makes the matching much more difficult. This unique feature is investigated here for the first time with an experimental structure whose fully integrate equivalent is depicted in Fig. 1(c). Measurements were performed using a single pH buffer (pH 8) to reveal the system transfer characteristics with each Fe-Cap and for different voltage pulse widths. Figure 1(d) shows the effect of three different pulse widths (10 μs, 100 μs, and 1 ms) on the I_D–V_G of our experimental structure using the PZT-Cap. No steepening in the subthreshold slope is observed for the longest pulses since the leakage current has time to discharge all the capacitors. On the other hand, very short voltage pulses (such as 10 μs) prevent the measurement of quasi-static transfer characteristics because of current overshoots, enhanced role of capacitance parasitics, and increased equivalent gate leakage in the subthreshold region.

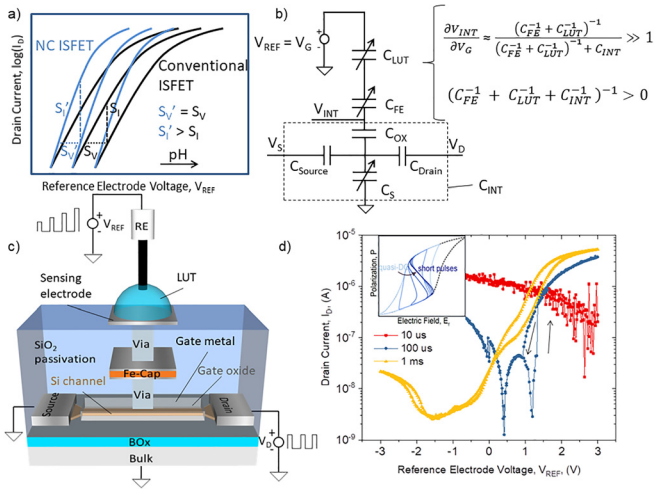

FIG. 1. (a) Expected qualitative characteristics of NC ISFET compared with a conventional ISFET. (b) NC ISFET capacitive divider, where a ferroelectric capacitor, C_{FE}, is connected in series with C_{LUT} and C_{MOS} to offer internal voltage gain under stabilized conditions. (c) Fully integrated equivalent of the structure of the experimental NC ISFET setup. In our experiments, the three main constituting elements (FD SOI transistor, Fe-Cap and sensing electrode) are externally connected. (d) Transfer characteristics of the LG NCFET embedding the single-crystalline Fe-Cap extracted with different pulse durations. The inset shows the qualitative effect of pulse duration on reaching the NC region of the polarization vs electric field curve.

For our NC ISFET devices, when the Fe-Cap is matched to the MOSFET capacitance, the optimal measurement conditions corresponded to a pulse duration on the order of 100 μs: when using such pulses, a clear subthermionic SS of 28 mV/dec over about two decades of I_D is observed.

Figure 2(a) compares double-sweep transfer characteristics extracted for this pulse duration from a NC ISFET embedding the High-Temperature (HT) Si:HfO_2-Cap (with an area of 100 × 100 μm^2) with the transfer characteristics of the baseline ISFET. The measured SS of the NC device is more than six times steeper than its conventional counterpart, achieving deep subthermionic value of 20 mV/dec over two decades of current and negligible hysteresis ≈ 2 mV. These parameters could offer a significantly improved S_I, with values up to 3 dec/pH, allowing one to precisely detect and measure extremely small pH variations.

The apparent leakage in pulsed measurements at $I_D \approx 30$ nA is due to the noise limit of the parameter analyzer.[36] Repeated measurements revealed some stability issues in this configuration, with shifts in V_{th} or the appearance of a hysteresis greater than 600 mV. This instability can be attributed to the parasitic capacitances in the setup due to external connectors and remote voltage amplifiers, which also affect the exact matching conditions.

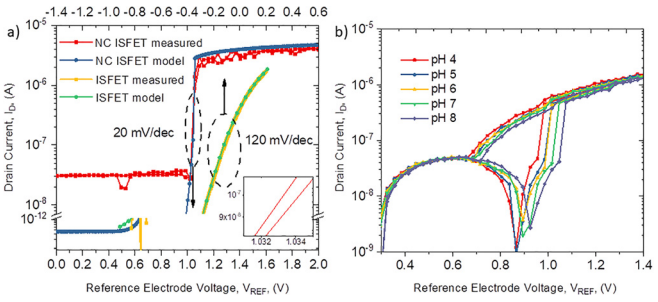

FIG. 2. (a) Comparison of the transfer characteristics of the baseline ISFET and NC ISFET embedding the HT Si:HfO_2-Cap extracted at 100 μs pulse duration, together with their corresponding simulation results. (b) Transfer characteristics of the LG NCFET embedding the LT Si:HfO_2-Cap extracted at different pH values.

Among the various Fe-Caps, the Low-Temperature (LT) Si:HfO_2-Cap appeared to have the most stable and repeatable behavior. While, similar to the case of the PZT LG NCFET, only one branch of the double-sweep transfer characteristics showed a remarkable steepening, we have been able to repeat the I_D–V_G measurements related to a given pH buffer multiple times without observing any relevant drift (see supplementary material). The transfer characteristics extracted with the full range of pH buffers (each measured three times) are shown in Fig. 2(b). The minimum SS is ≈27 mV/decade for all curves. The extracted voltage sensitivity, S_V, appears to be lower, 14 mV/pH, compared to the one of the baseline ISFET, which is coherent with the decrease in voltage sensitivity observed on ISFETs biased in pulsed mode (from 40 to 25 mV/pH using, respectively, measurements in DC and with 10 ms pulses). The further decrease to 14 mV/pH in the NC ISFET experiment is attributed to the shorter pulse duration used for their characterization. A V_{th} shift has been observed when repeating the measurement of a given pH buffer after completing the characterization. This suggests that instability effects could be superimposed to our pH-induced shifts.

Future implementations of bio-sensing systems based on NC FETs should consider two privileged directions: (1) the use NC FET devices architectures without metal plane between the ferroelectric and the gate oxide (to avoid high-instabilities and to make it easier to exploit a stable NC effect in DC measurements) and with the sensing electrodes functionalized as post-back-end-of-line (BEOL) process and (2) including both the ferroelectric and the functionalized electrodes in the BEOL process, with the advantage of a conventional CMOS transducing element but paying the price of instabilities and of additional parasitics for NC matching.

A compact physical model for NC FET, capable of calculating the gate charge density as a function of voltage, has been previously proposed[37] and will serve as a basis to build our model for a NC FET with a LG. The presence of a LG in the system requires an accurate description of the physics of the LUT since its capacitance will depend on several relevant factors, such as pH, ion concentrations, and RE bias. The physical model used in this work for the capacitance of the LG is based on the Stern model,[38] which describes the liquid in contact with a solid material as two different layers in series: a molecule-thin layer of ions immobilized on the surface, the stern layer, and a thicker layer of liquid where ions are free to move, the diffuse layer, each having its own capacitance.

The complete analytical equations and parameters of the NC ISFET model are presented in the supplementary material, while the most relevant numerical results obtained after the calibration are reported in Fig. 3.

Figures 3(b) and 3(c) show the band diagrams of the standard ISFET and the NC ISFET at the same V_{REF}, taking into account the combined effects of LG and NC that clearly boosts the channel inversion level in Fig. 3(c). Most remarkable is that the Fe-Cap shows an opposite voltage drop with respect to the positive elements. Here, the bandgap of the LG has been assumed equal to zero in agreement with reported ISFET simulation parameters.[39]

Figure 3(d) illustrates that the capacitance of the stern layer (C_{stern}) is mostly independent of V_{REF} and of the pH, coherently with the assumptions of the stern model. The capacitance of the diffuse layer (C_{diff}) here is almost one order of magnitude lower than C_{stern} but its magnitude is highly dependent on the concentration of free ions in the LUT (∼6 × 10^{25} m^{-3}, equivalent to 100 mM concentration). For different ion concentrations, the ratio between these two capacitances will change accordingly. The NC ISFET model introduces an additional variable Fe-Cap between the FD SOI MOSFET and the LG capacitor, with respect to the ISFET model. The complete system is modeled using the Landau–Devonshire model of a Si-doped HfO_2 Fe-Cap having a thickness of 16 nm, a residual polarization of 11.5 $\mu C/cm^2$, and a critical bias of 1.2 V, in agreement with our experimental characterization.

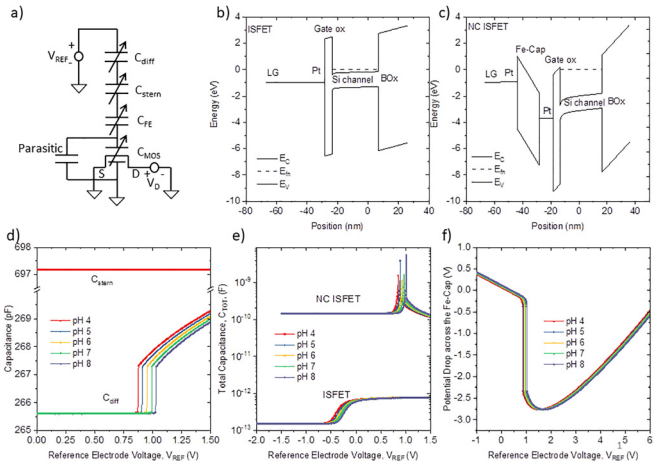

FIG. 3. (a) Equivalent capacitive circuit of the simulated NC ISFET. (b) ISFET band diagram at $V_{REF} = 1$ V. (c) NC ISFET band diagram at $V_{REF} = 1$ V. (d) C–V characteristics of the diffuse and stern layers for different pH values in NC configuration. (e) C–V characteristics of the baseline and NC ISFET for different pH values. (f) Potential drop across the Fe-Cap as a function of V_{REF} for different pH values.

The total capacitance simulations of NC ISFET in Fig. 3(e) correspond to the experimental I–V characteristics reported in Fig. 2(a), and the peaks in capacitance correspond to the achievement of complete matching. Furthermore, as mentioned, the dramatic increase in capacitance due to the NC effect, greater than two orders of magnitude here, would improve the signal-to-noise ratio of NC ISFET sensors by reducing the flicker noise.[40]

Finally, Fig. 3(f) shows the potential drop across Fe-Cap with respect to RE bias after finding a self-consistent solution of the capacitor divider. For a wide range of positive V_{REF}, the potential drop on the Fe-Cap is negative, meaning that it is operating as a voltage amplifier. The developed model for the NC ISFET not only gives a deeper insight into the dynamics of the capacitances but can also be used as a predictive tool for designing and optimizing further NC ISFETs.

In summary, we have reported the first experimental demonstration of an ISFET sensor with subthermionic transfer characteristics, showing an SS of 20 mV/decade over two decades of I_D, due to NC effect of Fe-Caps using Si-doped HfO_2. We have validated our experimental findings with calibrated simulations and have been able to obtain excellent agreement between the model and experimental data.

Overall, this work paves the way for further investigations using steep-slope devices for sensing analytes in biofluids with significantly higher current sensitivity.

See the supplementary material for detailed description of the model for capacitance, characterization of the UTB FD SOI ISFETs,

characterization of the Fe-Caps, study of the secondary effects of the pulsed mode measurements, study of the stability of the LT Si:HfO_2 ISFET, and the full list of physical parameters employed in our model.

This publication has received funding from the European Research Council (ERC) under the European Union's Horizon 2020 research and innovation programme, Grant Agreement No. 695459, Milli-Tech and from the Department of Science and Technology India–Swarnajayanti fellowship. The authors greatly appreciate the contributions of Robin Nigon and Paul Muralt in the fabrication of the single-crystalline PZT thin film and the help of Eamon P. O'Connor in the proofreading of the manuscript.

A reasonable minimal dataset supporting the findings of this study is available from the corresponding authors upon reasonable request.

REFERENCES

[1]E. Accastelli, P. Scarbolo, T. Ernst, P. Palestri, L. Selmi, and C. Guiducci, Biosensors **6**(1), 9 (2016).
[2]J. H. Ahn, J. Y. Kim, M.-L. Seol, D. J. Baek, Z. Guo, C. H. Kim, S. J. Choi, and Y. K. Choi, Appl. Phys. Lett. **102**(8), 083701 (2013).
[3]M. S. Andrianova, E. V. Kuznetsov, V. P. Grudtsov, and A. E. Kuznetsov, Biosens. Bioelectron. **119**, 48 (2018).
[4]E. M. Briggs, S. Sandoval, A. Erten, Y. Takeshita, A. C. Kummel, and T. R. Martz, ACS Sens. **2**(9), 1302 (2017).
[5]E. Buitrago, G. Fagas, M. F. B. Badia, Y. M. Georgiev, M. Berthom, and A. M. Ionescu, Sens. Actuators, B **183**, 1 (2013).
[6]E. Buitrago, M. F. B. Badia, Y. M. Georgiev, R. Yu, O. Lotty, J. D. Holmes, A. M. Nightingale, H. M. Guérin, and A. M. Ionescu, Sens. Actuators, B **199**, 291 (2014).
[7]S. Chen, J. G. Bomer, E. T. Carlen, and A. van den Berg, Nano Lett. **11**(6), 2334 (2011).
[8]E. Garcia-Cordero, F. Bellando, J. Zhang, F. Wildhaber, J. Longo, H. Guerin, and A. M. Ionescu, ACS Nano **12**(12), 12646 (2018).
[9]J. Go, P. R. Nair, Jr., B. Reddy, B. Dorvel, R. Bashir, and M. A. Alam, ACS Nano **6**(7), 5972 (2012).
[10]D. S. Juang, C. H. Lin, Y. R. Huo, C. Y. Tang, C. R. Cheng, H. S. Wu, S. F. Huang, A. Kalnistsky, and C. C. Lin, Biosens. Bioelectron. **117**, 175 (2018).
[11]M. Kaisti, Biosens. Bioelectron. **98**, 437 (2017).
[12]B. Khamaisi, O. Vaknin, O. Shaya, and N. Ashkenasy, ACS Nano **4**(8), 4601 (2010).
[13]T. C. Lin, Y. S. Li, W. H. Chiang, and Z. Pei, Biosens. Bioelectron. **89**, 511 (2017).
[14]S. Ma, X. Li, Y. K. Lee, and A. Zhang, Biosens. Bioelectron. **117**, 276 (2018).
[15]S. Nakata, T. Arie, S. Akita, and K. Takei, ACS Sens. **2**(3), 443 (2017).
[16]S. Park, M. Kim, D. Kim, S. H. Kang, K. H. Lee, and Y. Jeong, Biosens. Bioelectron. **147**, 111737 (2020).
[17]S. Rigante, P. Scarbolo, M. Wipf, R. L. Stoop, K. Bedner, E. Buitrago, A. Bazigos, D. Bouvet, M. Calame, C. Schönenberger, and A. M. Ionescu, ACS Nano **9**(5), 4872 (2015).
[18]M. Schwartz, T. C. Nguyen, X. T. Vu, M. Weil, J. Wilhelm, P. Wagner, R. Thoelen, and S. Ingebrandt, Phys. Status Solidi A **213**(6), 1369 (2016).
[19]A. P. Soldatkin, J. Montoriol, W. Sant, C. Martelet, and N. Jaffrezic-Renault, Biosens. Bioelectron. **19**(2), 131 (2003).
[20]M. Wipf, R. L. Stoop, A. Tarasov, K. Bedner, W. Fu, I. A. Wright, C. J. Martin, E. C. Constable, M. Calame, and C. Schönenberger, ACS Nano **7**(7), 5978 (2013).
[21]S. Zafar, C. D'Emic, A. Afzali, B. Fletcher, Y. Zhu, and T. Ning, Nanotechnology **22**(40), 405501 (2011).
[22]S. Zhao, C. Shi, H. Hu, Z. Li, G. Xiao, Q. Yang, P. Sun, L. Cheng, W. Niu, J. Bi, and Z. Yue, Biosens. Bioelectron. **151**, 111962 (2020).
[23]See https://www.thoughtco.com/definition-of-ph-in-chemistry-604605 for the definition of pH in chemistry (last accessed February 19, 2020).
[24]A. Kumar, P. P. Balakrishna, X. Song, and M. M. De Souza, ACS Appl. Mater. Interfaces **10**(23), 19812 (2018).
[25]S. Salahuddin and S. Datta, Nano Lett. **8**, 405 (2008).
[26]Q. Xu, X. Liu, B. Wan, Z. Yang, F. Li, J. Lu, G. Hu, C. Pan, and Z. L. Wang, ACS Nano **12**(9), 9608 (2018).
[27]J. Zhou, J. Wu, G. Han, R. Kanyang, Y. Peng, J. Li, H. Wang, Y. Liu, J. Zhang, Q. Sun, Y. Hao, and D. W. Zhang, in *2017 IEEE International Electron Devices Meeting (IEDM)* (IEEE, 2017), p. 15.
[28]J. Jo, W. Y. Choi, J. D. Park, J. W. Shim, H. Y. Yu, and C. Shin, Nano Lett. **15**(7), 4553 (2015).
[29]D. J. Appleby, N. K. Ponon, K. S. Kwa, B. Zou, P. K. Petrov, T. Wang, N. M. Alford, and A. O'Neill, Nano Lett. **14**(7), 3864 (2014).
[30]G. Anran, H. Qinghua, Z. Lantian, Z. Qingtai, L. Tie, and W. Yuelin, CN patent 108,231,901 (2018).
[31]S. S. Tan, K. B. E. Quek, E. H. Toh, and L. Wang, U.S. patent 10,495,603 B1 (2019).
[32]A. Saeidi, F. Jazaeri, F. Bellando, I. Stolichnov, G. V. Luong, Q. T. Zhao, S. Mantl, C. C. Ecnz, and A. M. Ionescu, IEEE Electron Device Lett. **38**(10), 1485 (2017).
[33]A. I. Khan, U. Radhakrishna, K. Chatterjee, S. Salahuddin, and D. A. Antoniadis, IEEE Trans. Electron Devices **63**(11), 4416 (2016).
[34]K. Ng, S. J. Hillenius, and A. Gruverman, Solid State Commun. **265**, 12 (2017).
[35]M. Hoffmann, F. P. Fengler, M. Herzig, T. Mittmann, B. Max, U. Schroeder, R. Negrea, P. Lucian, S. Slesazeck, and T. Mikolajick, Nature **565**(7740), 464 (2019).
[36]See https://nanohub.org/resources/10523/download/2010.11.11-L12-Keithley.pdf for information on the minimum measurable current at a given frequency with Keithley parameter analyzer (last accessed January 20, 2020).
[37]G. Pahwa, T. Dutta, A. Agarwal, and Y. S. Chauhan, IEEE Trans. Electron Devices **64**(3), 1366 (2017).
[38]O. Stern, Z. Elektrochem. Angew. Phys. Chem. **30**(21-22), 508 (1924).
[39]A. Bandiziol, P. Palestri, F. Pittino, D. Esseni, and L. Selmi, IEEE Trans. Electron Devices **62**(10), 3379 (2015).
[40]N. Zagni, P. Pavan, and M. A. Alam, Appl. Phys. Lett. **114**(23), 233102 (2019).